

Differences Between Hole and Electron Doping of a Two-Leg CuO Ladder

S. Nishimoto* and E. Jeckelmann†

Philips-Universität Marburg, Fachbereich Physik, D-35032 Marburg, Germany

D.J. Scalapino‡

Department of Physics, University of California

Santa Barbara, California 93106-9530

(Dated: November 6, 2018)

Here we report results of a density-matrix-renormalization-group (DMRG) calculation of the charge, spin, and pairing properties of a two-leg CuO Hubbard ladder. The outer oxygen atoms as well as the rung and leg oxygen atoms are included along with near-neighbor and oxygen-hopping matrix elements. This system allows us to study the effects of hole and electron doping on a system which is a charge transfer insulator at a filling of one hole per Cu and exhibits power law, d -wave-like pairing correlations when doped. In particular, we focus on the differences between doping with holes or electrons.

PACS numbers: 71.10.Fd, 74.20.Mn, 71.10.Li

I. INTRODUCTION

Two-leg CuO ladder materials are known to exhibit some of the basic physical properties of the high T_c cuprates. Undoped two-leg ladder materials are found to be spin-gapped, charge transfer insulators^{1,2} and superconductivity has been observed in hole-doped ladders under high pressure.^{3,4,5} Moreover, ladder models have proved amenable to numerical studies, allowing one to explore the relationship between the parameters in the model and physical properties such as the charge and spin gaps of the insulating state and the pairing correlations in the doped state.^{6,7} Here we continue this type of theoretical study by examining the properties of a CuO ladder using a density-matrix-renormalization-group (DMRG) analysis.⁸ We will focus on the differences between hole and electron doping.

The geometry of the two-leg ladder which we will study is illustrated in Fig. 1. The Cu sites are characterized by a $d_{x^2-y^2}$ orbital, the rung O sites by a p_y orbital, and the leg O sites by a p_x orbital. The hole Hamiltonian for this model is given by

$$\begin{aligned}
 H = & \Delta_{pd} \sum_{i\sigma} p_{i\sigma}^\dagger p_{i\sigma} - t_{pd} \sum_{\langle ij \rangle \sigma} \left(d_{i\sigma}^\dagger p_{j\sigma} + p_{j\sigma}^\dagger d_{i\sigma} \right) \\
 & - t_{pp} \sum_{\langle ij \rangle \sigma} \left(p_{i\sigma}^\dagger p_{j\sigma} + p_{j\sigma}^\dagger p_{i\sigma} \right) \\
 & + U_d \sum_i d_{i\uparrow}^\dagger d_{i\uparrow} d_{i\downarrow}^\dagger d_{i\downarrow} + U_p \sum_i p_{i\uparrow}^\dagger p_{i\uparrow} p_{i\downarrow}^\dagger p_{i\downarrow} \quad (1)
 \end{aligned}$$

Here t_{pd} is the one-hole hopping matrix element between nearest-neighbor Cu and O sites and the first sum in Eq. (1) is over all nearest-neighbor sites. We will assume for simplicity that t_{pd} has the same value between all the Cu and O sites. The second term in Eq. (1) sums over all nearest-neighbor pairs of O sites and t_{pp} is the hopping matrix elements between these sites. We have chosen the

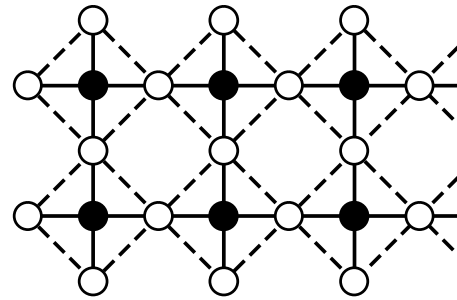


FIG. 1: Schematic lattice structure of a two-leg CuO ladder. Here the solid circles represent $\text{Cu}(d_{x^2-y^2})$ orbitals and the open circles represent $\text{O}(p_y)$ orbitals on the rungs and $\text{O}(p_x)$ orbitals on both legs. The orbital phases are chosen so that there is a hopping matrix element t_{pd} between nearest-neighbor Cu and O sites represented by the solid lines and a hopping matrix element t_{pp} between nearest-neighbor O sites represented by the dashed lines.

phases of the orbitals such that the signs of the hopping matrix elements are constant and with the minus sign convention of Eq. (1), $t_{pd} > 0$ and $t_{pp} \geq 0$. The energy difference between the O and Cu sites is $\Delta_{pd} = \epsilon_p - \epsilon_d > 0$ and U_d , and U_p are the on-site Coulomb energies for Cu and O, respectively. In this model an undoped ladder corresponds to a density of one hole per Cu site. We will work in units where $t_{pd} = 1$ and take as typical values $U_d = 8$ and $U_p = 3$, throughout.

Two of the authors previously studied a similar model⁹ in which the outer O sites were missing and only the near-neighbor Cu-O hopping t_{pd} was present. While this simplified form allowed one to compare a charge-gap-insulator model with the traditional one-band Hubbard and t - J models, the absence of the outer O and the t_{pp} hoppings altered the electronic structure.^{10,11} In addition, the electron-doped pairing response of the model appeared to be quite different from the hole-doped be-

havior. Here, for the more realistic structure shown in Fig. 1, we return to the study of the two-leg CuO ladder in which the charge-transfer nature of the insulating state is treated along with the effects of the oxygen t_{pp} hopping matrix elements. We also will study longer ladders with up to 32×2 Cu atoms corresponding to 226 total O and Cu sites.

We calculate the static properties of the model (1) numerically using the DMRG method.⁸ With this approach we obtain accurate ground state energies and expectation values (such as correlation functions) for a fixed number of holes of each spin. In the DMRG calculations, open-end boundary conditions are used so that when we discuss local quantities they will actually be averaged over the ladder and correlation functions will be calculated using distances taken about the midpoint. We have used up to $m = 2000$ density matrix eigenstates to build the DMRG basis. Using an extrapolation of DMRG ground state energies to vanishing discarded weight,¹² we have obtained ground state energies and gaps which are accurate to parts in $10^{-3}t_{pd}$. Although the largest source of errors in our calculations are finite size effects, we have been able to extrapolate a number of gap measurements to an infinite-size ladder.

In Sec. II we discuss our results for a filling of one hole per Cu, which corresponds to the undoped ladder. Our main interest is in the effect of the site energy difference $\Delta_{pd} = \epsilon_p - \epsilon_d$ and the oxygen hopping parameter t_{pp} . We will examine the charge and spin magnitudes on the various sites and the dependence of the charge and spin gaps on Δ_{pd} and t_{pp} . When U_d is large compared with Δ_{pd} and $\Delta_{pd} \gtrsim 2t_{pp}$, we find as expected that the ladder is a charge transfer insulator with a spin gap. By comparing the low-lying spin states of the CuO model with a two-leg Heisenberg model, we extract effective rung and leg exchange interactions. In Sec. III, we examine the charge and spin magnitude distributions for the doped case and find that, for typical parameters characteristic of the cuprates, the doped holes tend to be spread out on the O lattice while doped electrons tend to be localized on the Cu sites. We also study the effect of doping on the effective exchange interactions and on the local spin-spin correlations. We then turn to a study of the pairing correlations for both the hole-doped and the electron-doped ladder. We find a power law behavior with negative “ d -wave-like”, Cu rung-leg pair correlations for both hole and electron doping. However, we find that the internal structure of a pair depends upon whether the system is electron- or hole-doped. In Sec. IV, we conclude with some further comments relating these results to the general problem posed by the cuprate materials.

II. THE UNDOPED LADDER

We first investigate the properties of an undoped ladder. For local properties such as the charge and spin magnitude distributions on the sites and the spin corre-

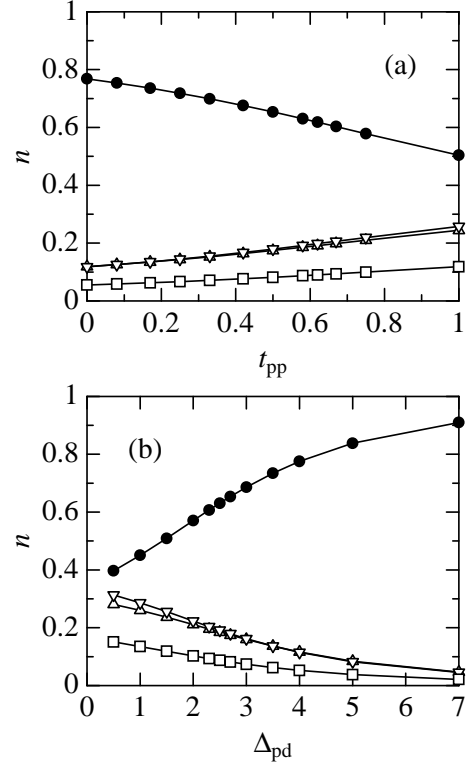


FIG. 2: Hole density $\langle n_{Cu} \rangle$ and $\langle n_O \rangle$ on the various sites of an undoped ladder with 8×2 Cu atoms: Cu sites (solid circles), rung O(p_y) sites (up-triangles), leg O(p_x) sites (down-triangles), and outer O sites (squares) versus (a) t_{pp} for $\Delta_{pd} = 2.7$ and (b) Δ_{pd} for $t_{pp} = 0.5$.

lations between sites, a ladder containing 8×2 Cu sites is sufficiently long. In Fig. 2 we show the average ground state hole occupation of Cu sites $\langle n_{Cu} \rangle = \langle d_{i\uparrow}^\dagger d_{i\uparrow} + d_{i\downarrow}^\dagger d_{i\downarrow} \rangle$ and of the various O sites $\langle n_O \rangle = \langle p_{i\uparrow}^\dagger p_{i\uparrow} + p_{i\downarrow}^\dagger p_{i\downarrow} \rangle$ as a function of t_{pp} and Δ_{pd} . In Fig. 2(a) the hole occupation is shown for $\Delta_{pd} = 2.7$ versus t_{pp} . As t_{pp} increases the hole occupation on the Cu sites decreases and that on the O sites increases. In Fig. 2(b), the hole occupation is shown for $t_{pp} = 0.5$ versus Δ_{pd} . Here as Δ_{pd} increases, the hole occupation on the Cu sites increases as one would expect. The hole occupation on the outer O sites is typically about half that on the other O sites. For $t_{pp} = 0.5$ and $\Delta_{pd} = 3$, the holes are approximately 70% on the Cu sites and 30% on the O sites.

The average value of the square of the spin moment

$$\langle \mathbf{S}_i^2 \rangle = \frac{1}{4} \left\langle \left(\Psi_{i\alpha}^\dagger \boldsymbol{\sigma}_{\alpha\beta} \Psi_{i\beta} \right)^2 \right\rangle \quad (2)$$

on various sites is shown in Fig. 3 for the same parameters. Here $\Psi_{i\alpha}^\dagger = d_{i\alpha}^\dagger$ or $p_{i\alpha}^\dagger$ depending upon the site, $\boldsymbol{\sigma}$ is the usual Pauli spin matrix, and the indices α and β are summed over. For $\Delta_{pd} = 3$ and $t_{pp} = 0.5$, the average spin moment on the Cu site is 0.5. Dividing this by the average hole occupation for the Cu gives a squared spin moment of order 0.7 compared with 3/4 for a Heisenberg

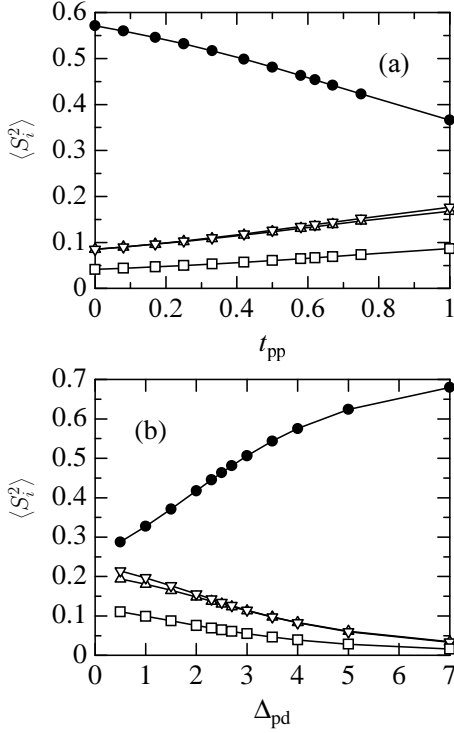


FIG. 3: Local spin moment $\langle S_i^2 \rangle$ on the various types of sites of an undoped ladder with 8×2 Cu atoms: Cu sites (solid circles), rung O(p_y) sites (up-triangles), leg O(p_x) sites (down-triangles), and outer O sites (squares) versus (a) t_{pp} for $\Delta_{pd} = 2.7$ and (b) Δ_{pd} for $t_{pp} = 0.5$.

spin $s = 1/2$. With $U_d = 8$, the spin moment is well formed on the Cu site and $\langle S_{\text{Cu}}^2 \rangle$ simply tracks $\langle n_{\text{Cu}} \rangle$, the probability of having a hole on a Cu site.

The charge gap of an undoped ladder with $L \times 2$ Cu sites is given by

$$\Delta_c(L) = E_0(+2, L) + E_0(-2, L) - 2E_0(0, L), \quad (3)$$

where $E_0(N, L)$ denotes the ground state energy of a ladder of length L with $N + 2L$ holes. Extrapolating the charge gap from numerical data for up to $L = 16$, we find the results for $\Delta_c(L \rightarrow \infty)$ plotted in Fig. 4. Here Fig. 4(a) shows $\Delta_c(L \rightarrow \infty)$ versus t_{pp} for various values of Δ_{pd} and Fig. 4(b) shows $\Delta_c(L \rightarrow \infty)$ versus Δ_{pd} for various values of t_{pp} . From these results, we see that in order to have a charge gap, we need $\Delta_{pd} \gtrsim 2t_{pp}$. Experimentally^{13,14}, Δ_c is of order 1.4 to 2 eV. If we take $t_{pp} \sim t_{pd}/2$ then $\Delta_{pd} \approx 3$ gives a realistic charge gap with $t_{pd} \approx 1.6$ eV.¹⁰

The lowest triplet spin excitation is gapped and localized on the Cu sites of the ladder (i.e., the spin density remains zero on the O sites in the triplet state). The spin gap is given by

$$\Delta_s(N, L) = E_0\left(\frac{N}{2} + 1, \frac{N}{2} - 1, L\right) - E_0\left(\frac{N}{2}, \frac{N}{2}, L\right), \quad (4)$$

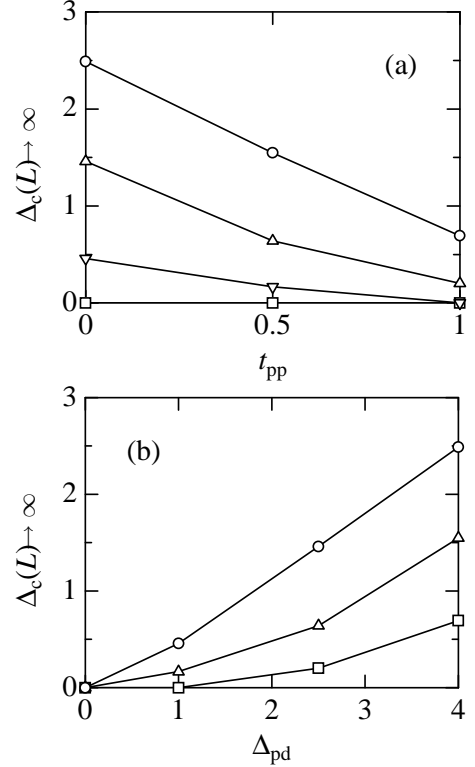


FIG. 4: Charge gap of undoped ladders extrapolated to an infinite ladder length $L \rightarrow \infty$. (a) As a function of t_{pp} for $\Delta_{pd} = 0$ (squares), $\Delta_{pd} = 1$ (down triangles), $\Delta_{pd} = 2.5$ (up triangles), and $\Delta_{pd} = 4$ (circles). (b) As a function of Δ_{pd} for $t_{pp} = 0$ (circles), $t_{pp} = 0.5$ (triangles), and $t_{pp} = 1$ (squares).

where $E_0(N_\uparrow, N_\downarrow, L)$ is the ground state energy of an $L \times 2$ ladder with $N_\sigma + L$ holes of spin $\sigma = \uparrow, \downarrow$. We first discuss the spin gap of the undoped ladder ($N = 0$). In this case we extrapolate the spin gap to an infinite ladder length using data for up to $L = 16$. The dependence of the spin gap $\Delta_s(L \rightarrow \infty)$ on t_{pp} and Δ_{pd} is shown in Figs. 5(a) and 5(b), respectively. As for the charge gap, there is a spin gap only if $\Delta_{pd} \gtrsim 2t_{pp}$. For large Δ_{pd} the spin gap decreases due to a decrease in the effective exchange coupling as observed in our previous work.⁹ Thus the spin gap goes through a maximum at a finite value of $\Delta_{pd} > 2t_{pd}$. Experimentally,^{6,10} $\Delta_s \sim 0.03 - 0.05$ eV so that with $t_{pd} \approx 1.6$ eV, we need $\Delta_s/t_{pd} \simeq 0.03$. This confirms that $t_{pp} \simeq 0.5$ and $\Delta_{pd} \simeq 3$ represent appropriate choices, consistent with electronic band structure calculations.¹⁰

For a two-leg Heisenberg ladder, the spin gap is equal to approximately half of the exchange interaction. Thus from Fig. 5(a) we see that provided $\Delta_{pd} \gtrsim 2t_{pp}$, the effective exchange interaction between Cu spins increases with t_{pp} . For example for $\Delta_{pd} = 2.5$, the spin gap and hence the effective Cu-Cu exchange increase by 40 % as t_{pp} goes from 0 to 0.5. This is due to the additional exchange path through the O ions. This crucial role of the O-O hopping t_{pp} in giving a large effective Cu-Cu exchange has been emphasized by Eskes and Jefferson.¹⁵

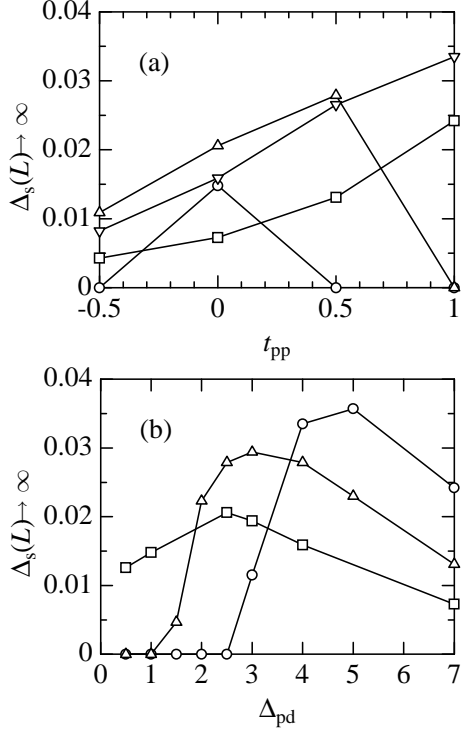


FIG. 5: Spin gap of undoped ladders extrapolated to an infinite ladder length $L \rightarrow \infty$. (a) As a function of t_{pp} for $\Delta_{pd} = 1$ (circles), $\Delta_{pd} = 2.5$ (up triangles), $\Delta_{pd} = 4$ (down triangles), and $\Delta_{pd} = 7$ (squares). (b) As a function of Δ_{pd} for $t_{pp} = 0$ (squares), $t_{pp} = 0.5$ (up triangles), and $t_{pp} = 1$ (circles).

The nearest-neighbor Cu spin-spin correlations $\langle \mathbf{S}_i \cdot \mathbf{S}_j \rangle$ are antiferromagnetic in the undoped ladder. For a fixed value of t_{pp} , $-\langle \mathbf{S}_i \cdot \mathbf{S}_j \rangle$ increases with Δ_{pd} and tends to the value obtained for a two-leg Heisenberg ladder when $\Delta_{pd} \gg t_{pp}$. This simply reflects the fact that increasing Δ_{pd} causes the holes to become more localized on the Cu sites, as shown by the increase of the Cu spin moments $\langle \mathbf{S}_i^2 \rangle$ in Fig. 3(b). For the same reason, for a fixed value of Δ_{pd} , $-\langle \mathbf{S}_i \cdot \mathbf{S}_j \rangle$ decreases with increasing t_{pp} and vanishes for $t_{pp} \gg \Delta_{pd}$. This decrease is due to the reduction of the local magnetic moments $\langle \mathbf{S}_i^2 \rangle$ on the Cu sites as the holes spread further onto the O sites, as seen in Fig. 3(a).

The low energy properties of the spin degrees of freedom of the undoped *d-p* Hubbard model (1) can be mapped onto an anisotropic Heisenberg ladder.

$$H = \sum_{\langle ij \rangle} J_{ij} \mathbf{S}_i \cdot \mathbf{S}_j . \quad (5)$$

Here $\langle ij \rangle$ represent near-neighbor bonds along the legs and rungs of a 2-leg ladder with $J_{ij} = J_{\perp}$ for the rungs and J_{\parallel} for the legs. To estimate the parameters J_{\perp} and J_{\parallel} , we consider the low-energy states of the *d-p* model for a $\text{Cu}_{2L}\text{O}_{5L}$ cluster ($L \times 2$ Cu ladder). Then by making a one-to-one correspondence of the states of this system to the $L \times 2$ Heisenberg ladder, we derive

the J_{\perp} and J_{\parallel} parameter of the anisotropic Heisenberg Hamiltonian. These processes are performed for ladders of length $L = 8, 12$, and 16 with the open boundary condition. We confirm that the low-lying spin states of the *d-p* and Heisenberg clusters have the same quantum numbers and characters for all the three values of L . To make the mapping systematically with various system sizes, we extract the two lowest triplet excitation energies, $E_{t1} = E_0(S_{\text{tot}} = 1) - E_0(S_{\text{tot}} = 0)$ and $E_{t2} = E_1(S_{\text{tot}} = 1) - E_0(S = 0)$. Here, $E_n(S = S_{\text{tot}})$ is the energy of the n^{th} excited state with total spin S . Then we determine J_{\perp} and J_{\parallel} by fitting the excitation energies E_{t1} and E_{t2} with results obtained from *d-p* clusters with the same L . In this way, with $\Delta_{pd} = 3$ and $t_{pp} = 0.5$, we find that $J_{\perp} = 0.06t_{pd}(\sim 96\text{meV})$ and $J_{\parallel} = 0.08t_{pd}(\sim 128\text{meV})$, both of which are in a reasonable range as compared to experimental and theoretical results.^{13,14,16}

It is also interesting to examine the effect of t_{pp} and Δ_{pd} on the effective exchange coupling anisotropy. From the nearest-neighbor Cu spin-spin correlation $\langle \mathbf{S}_i \cdot \mathbf{S}_j \rangle$ we define

$$R = \frac{\langle \mathbf{S}_i \cdot \mathbf{S}_j \rangle_{\text{rung}}}{\langle \mathbf{S}_i \cdot \mathbf{S}_j \rangle_{\text{leg}}}, \quad (6)$$

where we use an average of $\langle \mathbf{S}_i \cdot \mathbf{S}_j \rangle$ over the ladder. For a Heisenberg ladder (5) with an exchange coupling J_{\perp} on the rungs and J_{\parallel} on the legs, R versus J_{\perp}/J_{\parallel} is shown in Fig. 6(a). Various experimental and theoretical estimates^{13,14,16} suggest that values of J_{\perp}/J_{\parallel} ranging from 0.5 to 1.0 are appropriate for two-leg CuO ladders. Figure 6(a) shows that this corresponds to values of R varying from 0.6 to 1.2. The ratio R obtained for our CuO ladder are shown versus t_{pp} and Δ_{pd} in Figs. 6(b) and 6(c), respectively. We see that the exchange coupling anisotropy is again consistent with parameter values $\Delta_{pd} \approx 3$ and $t_{pp} \approx 0.5$. In the absence of the outer O sites, the anisotropy ratio R becomes significantly larger than the values shown in Figs. 6(b) and 6(c) for $0 < t_{pp} \leq 1$. In the charge transfer insulating phase, one finds an effective exchange coupling ratio $J_{\perp}/J_{\parallel} > 1$ for realistic parameters, in disagreement with most experimental and theoretical estimates. Thus, it appears that it is important to include the outer O sites in order to obtain a qualitatively correct description of two-leg CuO ladders.

The dependence of the charge and spin magnitude distributions, the charge and spin gaps, and the spin-spin correlations on the parameters t_{pp} and Δ_{pd} can be understood qualitatively. For $t_{pp} \gtrsim \Delta_{pd}/2$, the holes are delocalized on all Cu and O sites and the undoped CuO ladder is in a metallic phase. For $\Delta_{pd} \gtrsim 2t_{pp}$, the holes tend to be localized on the Cu sites and the undoped system is a charge-transfer insulator. Low-energy spin excitations involve the holes on the Cu sites only. Thus, the spin degrees of freedom localized on the Cu sites lead to an effective two-leg spin ladder. Here, as noted, we are working in units where $t_{pd} = 1$, $U_d = 8$, and $U_p = 3$. We have

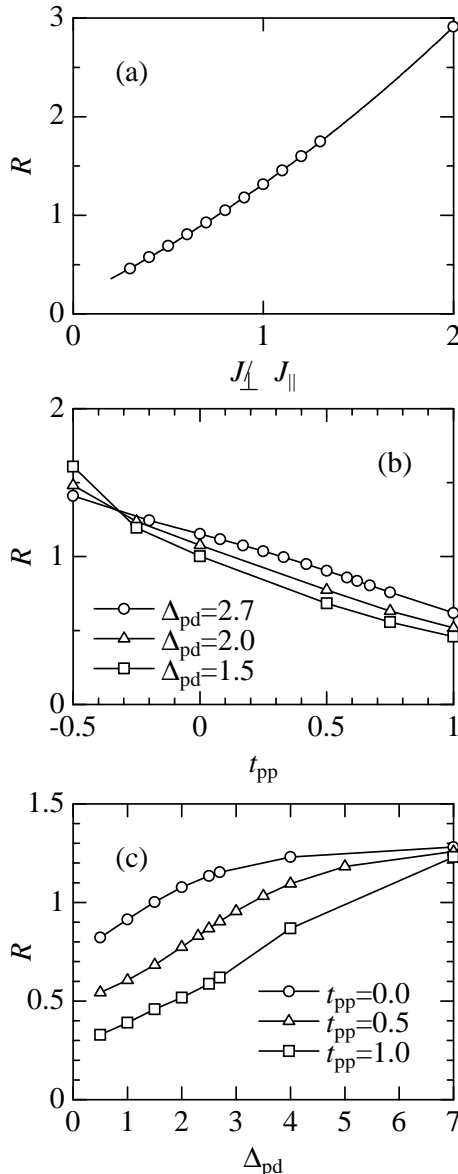


FIG. 6: Ratio R between nearest-neighbor spin correlations on rungs and legs. (a) For a two-leg Heisenberg ladder with 100 rungs as a function of J_{\perp}/J_{\parallel} . For an undoped CuO ladder with 8×2 Cu sites (b) versus t_{pp} and (c) versus Δ_{pd} .

seen that the magnitudes of the charge and spin gaps as well as the site charge densities, spin moments, and effective exchange couplings are consistent with $\Delta_{pd} = 3$ and $t_{pp} = 0.5$. We will now examine what happens when such a CuO ladder is doped with holes and electrons.

III. THE DOPED LADDER

Turning to the doped situation, we investigate the properties of the model (1) with $\Delta_{pd} = 3$, $U_d = 8$, $U_p = 3$, and $t_{pp} = 0.5$ for various hole concentrations (per Cu atom) $x = 1 + N/(2L)$, where N is the number of doped

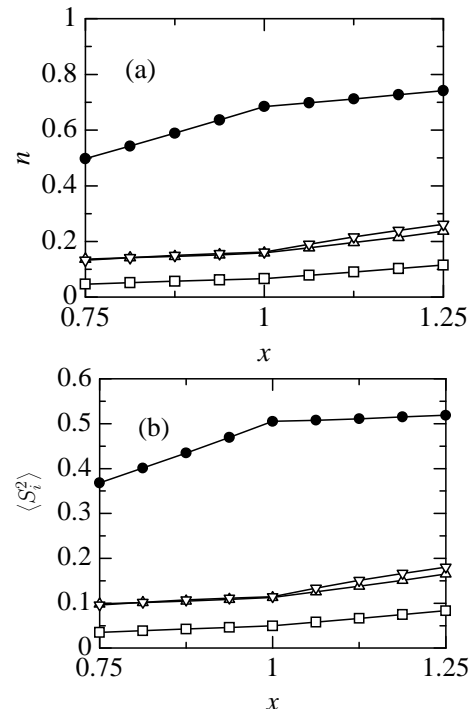


FIG. 7: (a) The hole density n and (b) the square of the spin moment $\langle S_i^2 \rangle$ on the various types of sites of a ladder with 16×2 Cu atoms as a function of filling x : Cu sites (solid circles), rung O(p_y) sites (up triangles), leg O(p_x) sites (down triangles), and outer O sites (squares).

holes ($N > 0, x > 1$) or doped electrons ($N < 0, x < 1$) in a ladder with $L \times 2$ Cu atoms. Results for the site occupations versus the doping are shown in Fig. 7(a). Here, we see that the slope of the hole occupation on the Cu site versus x changes at $x = 1$. For electron doping, the electrons are more likely to go on the Cu site than are the holes when the system is hole doped. This is, of course, what one would expect for a charge-transfer insulator. This is also consistent with Monte Carlo results for the 3-band Hubbard model^{17,18} as well as our previous DMRG results for the CuO ladder.⁹ The variation of the local squared spin moments on the different sites versus doping are shown in Fig. 7(b). As discussed previously, in the charge transfer regime, where U_d is large compared to Δ_{pd} and Δ_{pd} is larger than several times t_{pp} , the spin moments are mainly on the Cu sites. When the system is electron doped, the electrons go onto the Cu sites eliminating their moments. Thus, the average moment on the Cu sites depends upon x in the same way as the Cu site occupation $\langle n_{\text{Cu}} \rangle$, and $\langle S_{\text{Cu}}^2 \rangle / \langle n_{\text{Cu}} \rangle$ remains essentially constant, of order 0.7. The change in the average moment shown in Fig. 7(b) simply reflects the fact that for the electron-doped case, spin moments at individual Cu sites are removed when electrons are added to those sites. Likewise, for the hole-doped situation the average spin moment on the Cu sites increases only slightly as x increases and a few more Cu sites have holes.

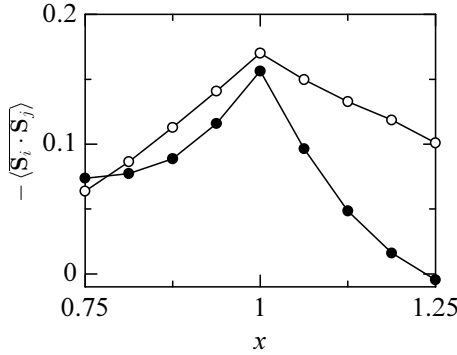


FIG. 8: The average nearest-neighbor Cu spin-spin correlation function $\langle \mathbf{S}_i \cdot \mathbf{S}_j \rangle$ on the rungs (solid circles) and legs (open circles) versus x calculated on ladders with 16×2 Cu sites.

In Fig. 8 we have plotted the average value of the nearest-neighbor Cu spin-spin correlations $\langle \mathbf{S}_i \cdot \mathbf{S}_j \rangle$ on the rungs and legs versus doping. As electrons are doped onto the ladder and spin moments are removed from the Cu sites, the magnitude of the $\langle \mathbf{S}_i \cdot \mathbf{S}_j \rangle$ correlations decrease on both the rungs and the legs. Similar results are observed for the nearest-neighbor spin-spin correlations in the $t - J$ model on a two-leg ladder as the hole concentration increases.

However, as holes are added to the CuO Hubbard model (1) and x increases, the rung spin-spin correlations decrease more rapidly than those along the legs. As we have seen, the added holes tend to go onto the O sites which frustrates¹⁹ or screens the exchange coupling between the Cu spins. A rough estimate of this can be seen by considering a Cu₄O₁₂ cluster with one hole or electron added. Calculating the low-lying states of the cluster and comparing the excitation energies with a 4-site t - J_{eff} system we find that J_{eff}/t_{pd} is 50% smaller for the one hole ($x = 1.25$) case relative to its value for the one electron ($x = 0.75$) case. Thus, in the hole-doped system, the effective exchange interaction between the spin moments on the Cu sites is weakened. Because this effective exchange is initially larger along the legs than across the rungs, the rung correlations decrease more rapidly than those along the legs. We note that the anisotropy in the reduction of the spin-spin correlations as a function of doping is much stronger than in a $t - J$ model on a two-leg ladder, even if one uses a strongly anisotropic exchange coupling $J_{\perp} \neq J_{\parallel}$.

The average values of the nearest-neighbor Cu-O spin-spin correlations increase rapidly with the number of holes in the ladder. For hole doping the appearance of strong nearest-neighbor Cu-O spin correlations corresponds to the formation of a Zhang-Rice singlet²⁰ in an isotropic two-dimensional CuO₂ lattice. In the two-leg CuO ladder, however, the strength of the Cu-O spin-spin correlation depends on the type of the O site considered. Rung Cu-O spin-spin correlations increase less rapidly than the other ones with increasing hole concentration

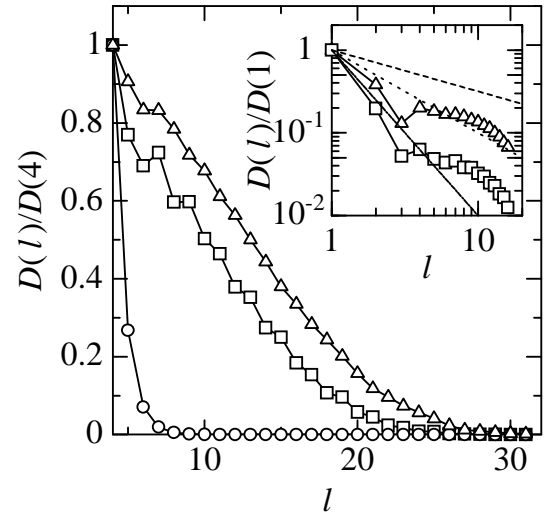


FIG. 9: The Cu rung-rung pair field correlation function $D(\ell) = \langle \Delta_{i+\ell} \Delta_i^\dagger \rangle$ versus ℓ for a 32×2 Cu ladder. Here, we have normalized $D(\ell)$ to its value at $\ell = 4$. Circles, squares, and triangles correspond to an undoped ladder, a ladder doped with two holes, and with two electrons, respectively. Inset: Same data (normalized to their $\ell = 1$ value) on a log-log scale. The lines have slope $-1/2$, -1 and -2 .

x . This confirms the higher frustration of antiferromagnetic correlations in the rung direction than in the leg direction when an additional hole is placed between the two holes localized on nearest-neighbor Cu sites. Correspondingly, for hole doping the spin-spin correlation between a Cu site and its outer O site increases faster than for the other nearest-neighbor sites because of the absence of frustration for this type of O sites.

Turning next to the pairing correlations, we have calculated the Cu rung-rung pair field correlation function

$$D(\ell) = \langle \Delta_{i+\ell} \Delta_i^\dagger \rangle \quad (7)$$

with

$$\Delta_i^\dagger = d_{i1\uparrow}^\dagger d_{i2\downarrow}^\dagger - d_{i1\downarrow}^\dagger d_{i2\uparrow}^\dagger. \quad (8)$$

Here, $d_{i\lambda s}^\dagger$ creates an electron of spin s on the i^{th} rung and the $\lambda = 1$ or 2 leg of the ladder. The pair field has “ d -wave-like” structure in the sense that the rung-leg Cu-Cu pair field correlation function, has a negative sign while the rung-rung or leg-leg pairing correlations are positive. We have also examined other pair field correlation functions corresponding to pairs on diagonal Cu sites or pairs on O sites and found that they are either qualitatively similar to the Cu rung-rung pair field correlations or decrease much faster. Some results for the rung-rung pair field correlation function $D(\ell)$ versus ℓ are shown in Fig. 9 for a ladder containing 32×2 Cu sites. We have normalized $D(\ell)$ with respect to its value at $\ell = 4$. The pair field correlations in the undoped system decay rapidly (exponentially) with distance while, as shown in the inset, the pair correlations when two electrons are added or

removed exhibit an approximate power law decay. (Qualitatively similar pair field correlation functions have been calculated in a $t-J$ two-leg ladder with two doped holes.) While the decay of the normalized rung-rung pair field correlations for the 2-electron and 2-hole doped ladders are similar in the CuO Hubbard model (1), the size of the rung-rung Cu pairing correlations are a factor of order 4 larger for the electron-doped case relative to the hole-doped one. This reflects the fact that for electron doping, the added carriers go primarily onto the Cu sites while for hole doping they go primarily onto the O sites. For higher doping ($0.75 \leq x \leq 1.25$) the Cu rung-rung pair field correlations are very similar to those shown in Fig. 9 for doped holes or electrons.

To determine whether doped holes or electrons form bound pairs we have first calculated the binding energy of two doped holes and electrons. The pair binding energy is defined as

$$\Delta_{pb}(L) = 2E_0(\pm 1, L) - E_0(\pm 2, L) - E_0(0, L), \quad (9)$$

where $E_0(N, L)$ is the ground state energy of a ladder with $L \times 2$ Cu site and $N + 2L$ holes. We could not extrapolate $\Delta_{pb}(L)$ to the $L \rightarrow \infty$ limit because finite-size effects are too irregular. However, we have found that $\Delta_{pb}(L \rightarrow \infty)$ is certainly positive both for hole and electron doping. Therefore, we expect two doped holes or electrons to build a bound pair in the CuO Hubbard ladder for the parameters we use here. As in our previous work,⁹ the binding energy of two doped holes is of the order of the spin gap of the undoped ladder. For instance, for a 16×2 Cu site ladder we have obtained $\Delta_{pb} \approx 0.02t_{pd}$, to be compared with the spin gap $\Delta_s(L \rightarrow \infty) = 0.03t_{pd}$. The binding energy of two electrons, $\Delta_{pb} \approx 0.04t_{pd}$, is also of the order of the spin gap in the undoped ladder but twice as large as the hole pair binding energy. In our previous investigation of the two-leg CuO ladder⁹ we found a vanishing pair binding energy for electron doping. To understand this change we have calculated the pair binding energy as a function of the various model parameters in a ladder with 8×2 Cu sites. It appears that the difference between the present result and the previous one⁹ is due to the nearest-neighbor O hopping t_{pp} . In fact, $t_{pp} > 0$ is necessary to obtain a finite pair binding energy in the electron doped ladder. When the CuO model is reduced to a simple, one-band Hubbard model, $t_{pp} > 0$ leads to an effective next-near-neighbor hopping t' which favors pairing when the system is electron doped.²¹ In addition, as previously discussed, $t_{pp} > 0$ leads to an enhanced Cu-Cu effective exchange.

In order to have a more detailed picture of the difference between the electron- and hole-doped pairs, we have investigated their internal structure. In a $t-J$ model or a spin-fermion model, it is easy to measure correlations between doped charges because there are no other itinerant charges (i.e., there are no charge fluctuations in the undoped system). In the CuO Hubbard model (1), however, bare electron-electron and hole-hole correlation functions give little information about the correlations

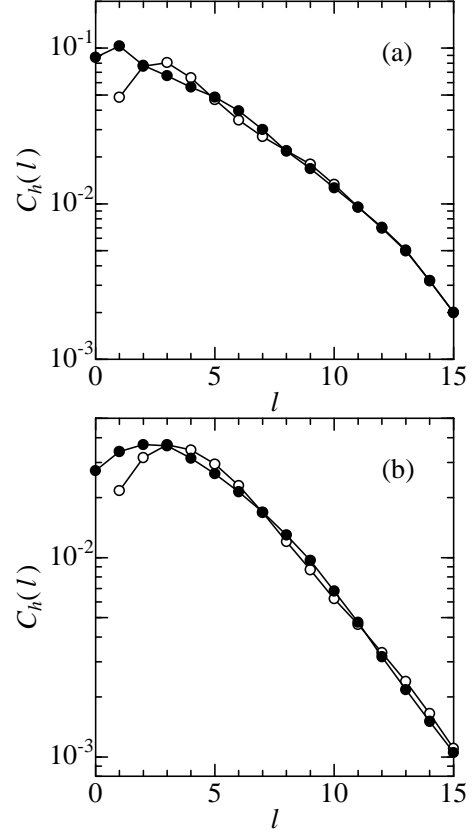


FIG. 10: The projected correlation functions $C_{e,h}(l)$ for (a) the Cu sites of a two-electron doped ladder and (b) the O₄ orbitals of a two-hole doped ladder. The distance l is measured along the ladder in units of the interval between two Cu rungs. Open and solid circles correspond to correlations between doped charges on the same leg and on different legs, respectively.

between two doped charges because they are dominated by the quantum fluctuations of the other charges. Therefore, we have to project out the ground state of (1) onto a subspace with no charge fluctuation. For that purpose we consider a perturbation expansion in t_{pd} and t_{pp} of the Hamiltonian (1) with $U_d > \Delta_{pd} > 0$ and x close to 1. The ground state of the unperturbed Hamiltonian ($t_{pd} = t_{pp} = 0$) is degenerate. For electron doping the ground state has at most one hole on each Cu site and no hole on any O site. The projection operator onto the ground-state subspace is

$$P_e = \prod_i (1 - d_{i\uparrow}^\dagger d_{i\uparrow} d_{i\downarrow}^\dagger d_{i\downarrow}) \prod_j (p_{j\uparrow}^\dagger p_{j\uparrow} p_{j\downarrow}^\dagger p_{j\downarrow}). \quad (10)$$

For hole doping there is exactly one hole on each Cu site and no doubly occupied O site in the ground state of the unperturbed Hamiltonian. The projection operator onto the ground-state subspace is

$$P_h = \prod_i (S_{i\uparrow}^d + S_{i\downarrow}^d) \prod_j (1 - p_{j\uparrow}^\dagger p_{j\uparrow} p_{j\downarrow}^\dagger p_{j\downarrow}), \quad (11)$$

where $S_{i\sigma}^d = d_{i\sigma}^\dagger d_{i\sigma} d_{i,-\sigma} d_{i,-\sigma}^\dagger$. Using perturbation theory one could then derive effective Hamiltonians (a generalized $t - J$ model and a generalized spin-fermion model, respectively) in the subspace defined by P_e and P_h , which approximately describe the low-energy properties of the CuO model (1) in the regime $t_{pd}, t_{pp} \ll \Delta_{pd} < U_d$ for electron doping and hole doping, respectively. Therefore, for the realistic parameters $\Delta_{pd} = 3t_{pd} = 6t_{pp}$, we calculate the ground state $|\psi\rangle$ of (1) and then use the projected states $P_e|\psi\rangle$ and $P_h|\psi\rangle$ to determine the correlations between doped carriers (electrons or holes).

Figure 10(a) shows the electron-electron correlation function

$$C_e^n(m) = \frac{\langle \psi | P_e E_n E_{n+m} P_e | \psi \rangle}{\langle \psi | P_e E_n P_e | \psi \rangle}, \quad (12)$$

where $E_n = d_{n\uparrow} d_{n\uparrow}^\dagger d_{n\downarrow} d_{n\downarrow}^\dagger$, calculated in a ladder with 32×2 Cu atoms and two doped electrons. $C_e^n(m)$ measures the correlation between two added electrons on the Cu sites. Note that the most probable arrangement for the two electrons is on diagonal nearest-neighbor sites, which is similar to what is seen in t-J ladders. Results for the hole-doped case are shown in Fig. 10(b). Here the hole-hole correlation function is given by

$$C_h^n(m) = \frac{\langle \psi | P_h \sum_{\sigma} H_{n\sigma} H_{n+m,-\sigma} P_h | \psi \rangle}{\langle \psi | P_h \sum_{\sigma} H_{n\sigma} P_h | \psi \rangle}, \quad (13)$$

where the operator

$$H_{n\sigma} = \frac{1}{4} \sum_{\langle nj \rangle} p_{j\sigma}^\dagger p_{j\sigma} \quad (14)$$

measures the probability of finding a hole in an O_4 orbital around the Cu site with index n (the sum runs over the four nearest-neighbor O sites of this Cu site). We average the density over four O sites around each Cu site because a doped hole is locked in a singlet state with another hole on a Cu site as in a CuO₄ cluster (i.e., in a Zhang-Rice singlet²⁰). This also facilitates the comparison with the electron-doped case and the $t - J$ two-leg ladder. $C_h^n(m)$ measures the correlation between two added holes in O_4 orbitals around different Cu sites. Figure 10(b) shows that the most probable arrangement for the holes is on diagonal next-nearest-neighbor O_4 orbitals.

For larger distance m , both $C_e^n(m)$ and $C_h^n(m)$ decrease approximately as $\exp(-|m|/\xi)$ with correlation lengths (in units of the distance between two Cu rungs) $\xi_e \approx 3.3$ and $\xi_h \approx 2.9$, respectively. Note that these correlation lengths cannot be interpreted as the pair size because the exponential decay sets in only for $m \gtrsim \xi_{e,h}$. The average distance between doped carriers is given by

$$\bar{m}_{e,h} = \frac{\sum_m |m| C_{e,h}(m)}{\sum_m C_{e,h}(m)}, \quad (15)$$

which yields $\bar{m}_e \approx 4.5$ and $\bar{m}_h \approx 4.8$ for the electron and hole pair, respectively.

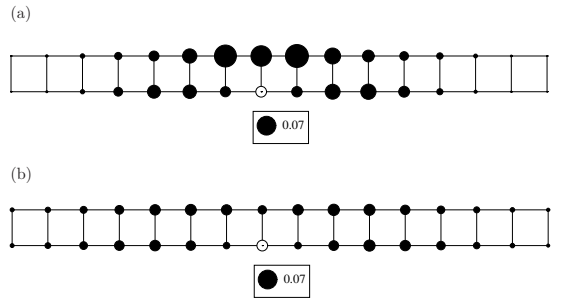


FIG. 11: A schematic view of the density-density correlations showing the structure of a pair in (a) an electron-doped ladder and (b) a hole-doped ladder. Here, one carrier (doped electron or hole) is located at the site n marked by an open circle (around the middle of the ladder). The radius of the solid circles is proportional to the probability $C_e^n(m)$ [$C_h^n(m)$] of finding the second doped electron (hole) on that site. Only the central part of ladders with 32×2 Cu sites is shown.

A more intuitive picture of the difference in the internal pair structure between electron and hole doping is shown in Fig. 11. Here, we show the probability $C_e(m)$ [$C_h(m)$] of finding the second doped electron (hole) at a Cu site (in a O_4 orbital) when the first doped electron (hole) is located on the Cu site (in the O_4 orbital) marked by an open circle. The electron pair appears to be denser than the hole pair which is qualitatively consistent with the larger binding energy (9) calculated for the electron-doped case.

As we use open boundary conditions, the correlation functions $C_{e,h}(m)$ depend on the position (i.e., the index n) of the first doped carrier (electron or hole). We have checked the pair structure for different ladder sizes and at different positions on the ladder and have found significant variations close to the ladder ends. In Fig. 11 we show the pair structure in the middle of a ladder with 32×2 Cu sites as finite-size and boundary effects are minimal there. We believe this structure to be representative of the pair structure in an infinite ladder.

As in the undoped ladder, the lowest triplet excitation in the doped ladder is gapped and involves only holes on the Cu sites. The spin gap (4) for the doped system versus x is shown in Fig. 12. Here, we have extrapolated the spin gap $\Delta_s(L)$ to $L \rightarrow \infty$ for fixed hole concentrations $x = 0, \pm 1/8$, and $\pm 1/4$ using numerical results for up to $L = 32$. For the limit $x \rightarrow 1$ we have extrapolated the spin gap $\Delta_s(L)$ to $L \rightarrow \infty$ for the 2-hole and the 2-electron doped ladders with up to $L = 32$. One sees that the value of the spin gap in the $x \rightarrow 1$ limit differs from the $x = 1$ undoped value. That is, the $q = (\pi, \pi)$ magnon in the undoped system ($x = 1$) has a gap of order 0.03, while in the doped system the spin gap as $x \rightarrow 1$ is of order 0.018. This behavior is similar to what has been found previously in studies of $t-t'-J$ ladders²².

An examination of the spin structure of the $S_z = 1$ state containing two doped electrons or holes shows that the spin and added carriers are spatially correlated.

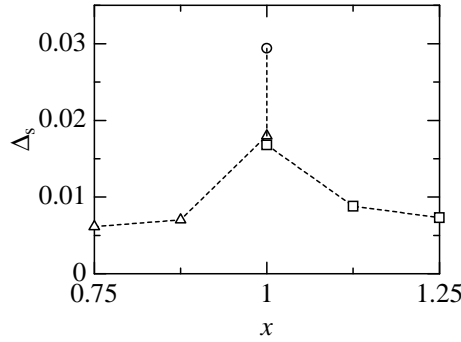


FIG. 12: The $L \rightarrow \infty$ extrapolated spin gap Δ_s versus hole concentration x . The open squares denote hole doping while the triangles denote electron doping. The undoped $x = 1$ case is shown as the open circle.

Thus, the spin gap is set by the energy of a bound magnon-carrier pair. For instance, Figure 13 shows the spin density (on the Cu sites) of the $S_z = 1$ state with two doped carriers (electrons or holes), when these doped carriers are in the configuration with the highest probability $C_{e,h}(m)$ (the pair structure of the triplet states is similar to that of the singlet states shown in Fig. 11). For electron doping, the spin structure shown in Fig. 13 is very similar to that found in $t-t'-J$ two-leg ladders.²² For hole doping, however, the spin structure is quite different, which is only in part due to the difference in the carrier configuration. Even if we use the same carrier configuration as for the electron-doped case (i.e., two doped carriers on nearest-neighbor diagonal sites), the spin structure of the hole-doped system is different from that found in the electron-doped system or $t-J$ model. In particular, we note that there is a small spin density on the Cu sites in the center of the O_4 orbitals where the holes are located, which shows that in the magnon-carrier pair, holes on Cu and O sites are no longer completely locked in a Zhang-Rice singlet.

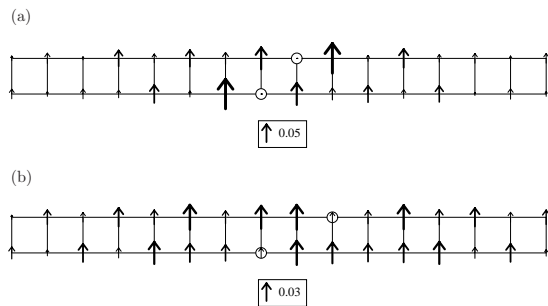


FIG. 13: A schematic view of a magnon in (a) an electron-doped ladder and (b) a hole-doped ladder. Here, both doped carriers (electrons or holes) are located at the positions (Cu sites or O_4 orbitals) marked by open circles around the middle of a ladder with 16×2 and 25×2 Cu sites, respectively. The length of the arrows is proportional to the spin density on the corresponding Cu site.

IV. CONCLUSION

Using the density matrix renormalization group, we have studied the structure of the charge, spin, and pairing correlations for a Hubbard-like model of a two-leg CuO ladder. This model allowed us to examine the differences between electron and hole doping that occur in a charge transfer insulator. For the undoped ladder, where there is one hole per Cu, we found that parameters obtained from LDA downfolding calculations^{10,11} lead to reasonable charge and spin gaps. A typical parameter set in units of the Cu-O hopping t_{pd} were a near-neighbor oxygen-oxygen hopping $t_{pp} = 0.5$, an oxygen-copper site energy difference $\Delta_{pd} = 3$, and on-site Cu and O Coulomb repulsions $U_d = 8$ and $U_p = 3$ respectively. With these parameters, the charge gap is determined primarily by Δ_{pd} rather than U_d and the spin gap is set by the effective Cu-Cu exchange. We have found that the O-O hopping t_{pp} plays a significant role in giving a large effective Cu-Cu exchange interaction.

For the undoped ladder, we found that the holes were distributed approximately 70% on the Cu sites and 30% on the O sites. The large on-site Coulomb interaction on the Cu site leads to the spin moment being dominantly on the Cu site. Basically, if the hole is on a Cu site, the square of the spin moment (0.7) has nearly its full value of 3/4. When electrons are added, they go primarily onto the Cu sites (of order 80% of the added charge goes onto the Cu sites). This is seen in both the decrease in the average Cu site hole occupation and the decrease in the average spin moment. Note that the decrease in the spin moment simply reflects the fact that there are fewer Cu^{++} sites in the electron-doped system. Alternatively, when holes are added (electrons are removed), they go primarily onto the O sites (of order 20% of the holes go onto the Cu with 80% going onto the surrounding O sites). This leaves the local spin moments on the Cu sites.

Thus, the undoped CuO ladder is a spin-gapped insulator with a charge gap set by the oxygen-copper site energy difference. Magnetically the undoped ladder is essentially a Heisenberg ladder made up of hole spins localized on the Cu sites. When the ladder is electron doped, some of the holes (and spins) on the Cu sites are removed and pairing correlations develop. Because the doped electrons go primarily onto the Cu sites, the electron-doped system is closer to the one-band Hubbard or $t-J$ models. When the ladder is hole doped, the holes go dominantly onto the O sites leading to a low-density gas of fermions delocalized over the O-site lattice and interacting by spin-exchange with the localized spins on the Cu sites. The local magnetic moments remain essentially unchanged on the Cu sites but the O holes frustrate the exchange coupling between the spins on the Cu sites.

This local, strong coupling picture focuses on the differences between the electron and hole-doped ladders. Nevertheless, on low energy scales, the spin gap and pairing correlations of the electron- and hole-doped systems

are quite similar. Both exhibit *d*-wave like power law pairing correlations in which the pair field Cu-Cu rung-leg correlations are negative. The spin gap for both dopings is associated with a bound magnon-pair. However, the internal structure of the pairs differ for electron and hole doping.

Acknowledgments

We would like to acknowledge useful discussions with O.K. Anderson, R. Martin, and G. Sawasky. DJS would

like to acknowledge support under a Department of Energy Grant No. DE-FG03-85ER-45197.

* E-mail: Satoshi.Nishimoto@Physik.Uni-Marburg.De
 † E-mail: Eric.Jeckelmann@Physik.Uni-Marburg.De
 ‡ Electronic address: djs@vulcan2.physics.ucsb.edu

¹ Z. Hiroi, M. Azuma, M. Takano, and Y. Bando, *J. Solid State Chem.* **95**, 230 (1991).
² M. Azuma, Z. Hiroi, M. Takano, K. Ishida, and Y. Kitaoka, *Phys. Rev. Lett.* **73**, 3463 (1994).
³ M. Uehara *et. al.*, *J. Phys. Soc. Jpn* **65**, 2764 (1996).
⁴ M. Isobe *et. al.*, *Phys. Rev. B* **57**, 613 (1998).
⁵ H. Mayaffre *et. al.*, *Science* **279**, 345 (1998).
⁶ E. Dagotto, *Rep. Prog. Phys.* **62**, 1525 (1999).
⁷ D.J. Scalapino and S.R. White, *Physica C* **341**, 367 (2000).
⁸ S.R. White, *Phys. Rev. B* **48**, 10345 (1993).
⁹ E. Jeckelmann, D.J. Scalapino, and S.R. White, *Phys. Rev. B* **58**, 9492 (1998).
¹⁰ O.K. Andersen, A.I. Liechtenstein, O. Jepsen, and F. Paulsen, *J. Phys. Chem. Solids* **65**, 1573 (1995).
¹¹ T.F.A. Müller *et. al.*, *Phys. Rev. B* **57**, R12655 (1998).
¹² For an example of this procedure, see J. Bonca, J.E. Gu-
 bernatis, M. Guerrero, E. Jeckelmann, and S.R. White, *Phys. Rev. B* **61**, 3251 (2000).
¹³ Z.V. Popovic *et. al.*, *Phys. Rev. B* **62**, 4963 (2000).
¹⁴ A. Gozar *et. al.*, *Phys. Rev. Lett.* **87**, 197202 (2001).
¹⁵ H. Eskes and J.H. Jefferson, *Phys. Rev. B* **48**, 9788 (1993).
¹⁶ C. de Graaf, I. de P.R. Moreira, F. Illas, and R.L. Martin, *Phys. Rev. B* **60**, 3457 (1999).
¹⁷ R.T. Scalettar, D.J. Scalapino, R.L. Sugar, and S.R. White, *Phys. Rev. B* **44**, 770 (1991).
¹⁸ G. Dopf, A. Muramatsu, and W. Hanke, *Phys. Rev. Lett.* **68**, 353 (1992).
¹⁹ A. Aharony *et. al.*, *Phys. Rev. Lett.* **60**, 1330 (1988).
²⁰ F.C. Zhang and T.M. Rice, *Phys. Rev. B* **37**, 3759 (1988).
²¹ S.R. White and D.J. Scalapino, *Phys. Rev. B* **60**, R753 (1999); G.B. Martins, J.C. Xavier, L. Arrachea, and E. Dagotto, *Phys. Rev. B* **64**, 180513 (2001).
²² D. Poilblanc *et. al.*, *Phys. Rev. B* **62**, R14633 (2000).